Noname manuscript No.
(will be inserted by the editor)

Quasi-linear viscoelastic model of the articular disc of the temporomandibular joint.

Maria S Commisso · Jose L Calvo-Gallego · Juana Mayo · Eiji Tanaka · Javier Martínez-Reina

Received: date / Accepted: date

Abstract A precise characterization of the articular disc of the temporomandibular joint (TMJ) is essential to study the masticatory biomechanics. The disc is responsible for the load distribution over the articular surface and for absorbing impacts during mastication. The main objective of this work is to characterize the mechanical behaviour of the articular disc under compression, the usual stress state during mastication. A quasi-linear viscoelastic (QLV) model, with a hyperelastic response for the elastic function, is proposed to describe the mechanical behaviour of the articular disc. The validity of that simplified model relies on the independence of their constants with the strain level and strain rate. The independence of the strain level was proved in a previous work. In this paper, different loading rates were tested to fully confirm the validity of the model in the physiological range of loads. Moreover, the strong non-linearity of the stress-strain relation made the exponential strain energy function the most suitable of the different models tried to represent the elastic response of the QLV model.

Keywords Articular disc · temporomandibular joint · stress relaxation test · quasi-linear viscoelasticity.

Maria S Commisso · Jose L Calvo-Gallego · Javier Martínez-Reina · Juana Mayo
Department of Mechanical Engineering, University of Seville, Camino de los Descubrimientos s/n E-41092 Seville, Spain
Tel.: +34-954481365
Fax: +34-954460475
E-mail: mcommisso1@us.es
Eiji Tanaka
Department of Orthodontics and Dentofacial Orthopedics, The University of Tokushima 11 Graduate School, Tokushima, Japan

1 Introduction

Disorders in the temporomandibular joint (TMJ) are very common and most of them are related to a malfunction of the articular disc [1]. The articular surfaces of the TMJ are highly incongruent, what could produce high contact loads in the articulating surfaces. The presence of the articular disc prevents high stresses by absorbing the loads and distributing them over larger contact areas.

In vivo measurements are difficult to perform in the articular disc, mainly due to the inaccessibility of the joint. Biomechanical models represent an alternative tool to study the TMJ, but it is important to have a proper constitutive models of the tissues involved and specially of the disc. This is also important in tissue engineering applications that require to mimic the mechanical behaviour of the joint. For instance, replacement of the articular disc has been proposed as a clinical solution for a large number of patients suffering from TMJ disc disorders [2].

The articular disc is a fibrocartilage made up of an extracellular matrix and variable amounts of cells. The matrix is composed of macromolecules (mainly type II collagen and proteoglycans) and interstitial fluid, representing $65-85\%$ of the wet weight of the disc [3]. Proteoglycans are hydrophilic molecules and, thus, cause an impedance to the fluid flow through the extracellular matrix. Fibrocartilage contains less proteoglycans than hyaline cartilage, thus facilitating the fluid flow. This fact allows simulating the behaviour of the first one with a viscoelastic model instead of more complex formulations like poroelastic or biphasic models, which rely upon modelling the drag force between the fluid and the solid matrix [4]. It is precisely the simplicity of viscoelastic models what makes them more interesting

than poroelastic models for modelling purposes and this is the principal aim of this paper: to propose a simple mechanical model and check whether it can still capture the behaviour of the TMJ disc.

The mechanical behaviour of the TMJ disc has been characterized in many studies. However, the test conditions varied greatly, including different species, strain rates and levels of strain or stress. Particularly, Chin et al. [5] evaluated the viscoelastic properties of human articular discs in compression by comparing the elastic moduli obtained at two different loading rates. They obtained an elastic modulus of 0.2 and 0.5 MPa for the loading rates of 0.04 mm/min and 0.08 mm/min, respectively. Beek et al. [6], performed dynamic indentation tests in human discs, at 3 positions in the anteroposterior axis, obtaining elastic moduli between 20 and 60 MPa depending on the analysed region. Later, del Pozo et al. [7] evaluated the viscoelastic properties of bovine discs in five areas, obtaining similar average moduli: anterior (17.4 MPa), central (15.7 MPa), posterior (16 MPa), lateral (14.7 MPa) and medial regions (14.4 MPa).

Several authors adjusted the relaxation curve obtained in compressive stress relaxation tests to a Kelvin model. For example, Tanaka et al. [8] did that in canine discs, obtaining the following mean values: instantaneous modulus $E_0 = 30.9$ MPa, relaxed modulus $E_\infty = 15.8$ MPa and relaxation time $\tau_1 = 31.2$ s. In bovine discs, del Pozo et al. [7] obtained the following ranges: $E_0 = 14.6 \div 17.3$ MPa, $E_\infty = 1.12 \div 2.32$ MPa and $\tau_1 = 6.2 \div 44.1$ s. Allen and Athanasiou [4] obtained the following ranges in porcine discs: $E_0 = 0.4 \div 1.9$ MPa, $E_\infty = 0.10 \div 0.17$ MPa and $\tau_1 = 32.5 \div 64.5$ s, with a great influence of the studied region. But, the region cannot explain by itself the great differences between their results and those obtained by the previous authors. The strain rate could also be behind such differences. For instance, del Pozo et al. [7] obtained higher elastic moduli than Allen and Athanasiou [4], but using higher strain rates.

This strain rate refers to the slope of the ramp applied in the relaxation test. Theoretically, a relaxation test imply the application of an instantaneous (Heaviside or step) strain. However, applying a step strain is impossible from a practical point of view, and even replacing the step by a very fast ramp is impractical since "transient stress waves will be induced in the specimens and a recording of the stress response will be confused by these elastic waves", as Fung states [9]. Instead, a ramp with a finite (though high) strain rate must be applied. The problem of doing this is that the viscoelastic constants could depend on the strain rate. That would reveal the necessity of a non-linear viscoelastic model and would be the case of the articular disc as appears from the referred results.

The strain rate is not the only influencing factor. Chin et al. [5] used strain rates much lower than Allen and Athanasiou [4], but obtained similar elastic moduli. This could be due to the non-linearity of the stress-strain relation and the different strain levels applied in the respective experiments. Such non-linearity, not considered by those authors, is another important factor to be addressed in the material model of articular discs. For example, Koolstra et al. [10] proposed a four-mode Maxwell model with the elastic part following a Mooney-Rivlin model and fitted the constants of the model from the shear dynamic tests performed by Tanaka et al. [11]. Lamela et al. [12] performed unconfined compression in porcine articular discs and fitted the results with Prony series in which the relaxation moduli were functions of the strain.

These previous results highlight the necessity of using nonlinear viscoelastic models to simulate the behaviour of articular discs. The aforementioned works used simple nonlinear viscoelastic models, as an alternative to the complex fully nonlinear models. Another alternative is the quasi-linear viscoelastic (QLV) model, proposed by Fung [9] and widely applied to soft tissues [9, 13–15], but not yet to TMJ discs, as far as we know. The advantage of the QLV model is that its constants can be fitted from relatively simple experiments, such as uniaxial compression. However, for the QLV model to be appropriate for a certain material, the constants fitted from experimental tests must be independent of the strain input (strain rate and maximum strain). In a previous work [16], it was seen that the maximum strain applied in stress relaxation tests did not affect those constants in the case of articular disc of pigs. However, the dependence of the QLV constants on the loading rate has not been checked yet.

The objective of this work is to describe the viscoelastic behaviour of the articular disc of pigs by performing stress relaxation tests at different strain rates. More precisely, the aim is to check the validity of a QLV model for that tissue, by showing the independence of its constants on the strain rate. Moreover, different hyperelastic models will be tried for the elastic part of the QLV model in order to choose the most appropriate one for this particular tissue.

2 Materials and methods

2.1 Extraction of samples

The articular discs were taken from *large white* pigs (aged from 8 months to 1 year) immediately after slaugh-

ter. A single cylindrical sample was extracted from the central region of each disc, where the thickness is more uniform (see figure 1). The samples were extracted in two phases: 1) using a hollow punch of 10 mm in diameter to allow the relaxation of prestresses, which deformed the sample, and 2) with a hollow punch of 5 mm to get an approximately circular cross section [17]. After extraction, the samples were photographed to measure their area through imaging techniques, so providing an equivalent diameter (ϕ_{eq}), given in table 1. The thickness of the samples was measured using optic microscopy at 8 points equally spaced over the periphery plus the middle point of each sample [17] (see fig. 2). The average of these 9 measurements were taken as the sample's thickness (L) and the difference between the maximum (L_{max}) and minimum thickness (L_{min}) was used to characterize the variation in thickness, ΔL. This variation must be small to ensure a uniaxial stress state, as established in a previous work [17]. In this work a criterion was established to reject those samples with an excessive ΔL, as a function of the diameter and the average thickness. This criterion was followed to finally accept 45 out of the 70 extracted samples.

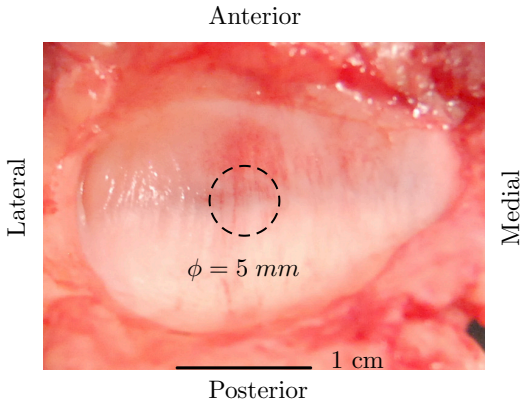

Fig. 1 Porcine articular disc of the temporomandibular joint, superior view. The region selected to extract the sample is indicated in dashed line.

Table 1 Dimensions (mean ± SD) of the cross sectional area, diameter, average thickness and variation in thickness measured in samples of porcine articular discs.

Area (mm^2)	ϕ_{eq}(mm)	L (mm)	ΔL (mm)
17.98 ± 1.81	4.78 ± 0.24	2.14 ± 0.43	0.53 ± 0.28

After extraction, the samples were individually: 1) wrapped in saline-soaked gauze, 2) enveloped in a plastic film and introduced in hermetic vials to prevent dehydration and 3) frozen at −20°C until testing. Based on previous studies, the viscoelastic properties of the samples are not affected by freezing if kept under these conditions [18, 19].

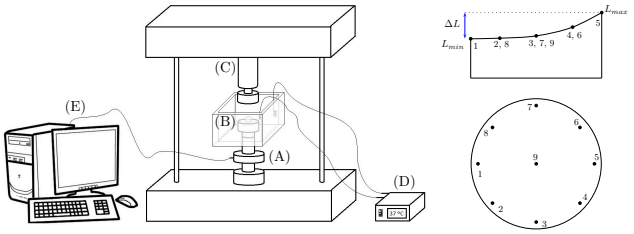

Fig. 2 Left: scheme of the testing device. (A) loading cell, (B) inferior platen, (C) upper platen; (D) temperature controlling system, (E) acquisition system. Right: schematic geometry of a real sample (solid line): lateral and upper view. The dots represent the points where the thickness of the sample was measured.

2.2 Test protocol

Apart from the uniformity of thickness, other test conditions with an influence on the stress state in the sample were studied in a previous work [20]: the portion of the specimen fixed to the platen and the friction coefficient between the platen and the non-fixed areas of the sample. The samples were fixed to the inferior platen with a circular piece of double-faced adhesive of 1 mm in diameter, stuck to the center of the sample. This size is small enough to achieve a stress state close to uniaxial in samples of diameter 5 mm [20]. In addition, vaseline was spread on the surface of both platens to reduce the friction in the non-fixed areas, as recommended in [20]. A servo-hydraulic testing machine (858 Mini Bionix II, MTS) was used for the tests. In figure 2 a schematic representation of the testing device is shown.

The samples were tested the day after extraction. First, they were submerged in saline solution at room temperature and allowed to thaw. Next, they were fixed to the inferior platen of the testing machine while submerged in a recipient containing saline at 37 ± 1 ° C. This temperature was controlled with a heater and thermostat. Before starting the test, the sample was allowed to reach that temperature during 15 minutes. Following, the upper platen was slowly lowered, approaching the sample, until the distance between the platens was equal to the average thickness of the sample, measured after extraction. The relative displacement was zeroed this position. A preconditioning was applied to each sample: 20 cycles from 0% to 10% strain at 1 Hz, like in [4]. The preconditioning was followed by a ramp from 0% to 50% strain and this final strain was maintained

for $15\,min$, for stress relaxation (see fig. 3). Stresses were recorded during the ramp and stress relaxation. Three different strain rates of the loading ramp were tested: 30, 40 and 50% strain per second [4], testing 15 samples in each case.

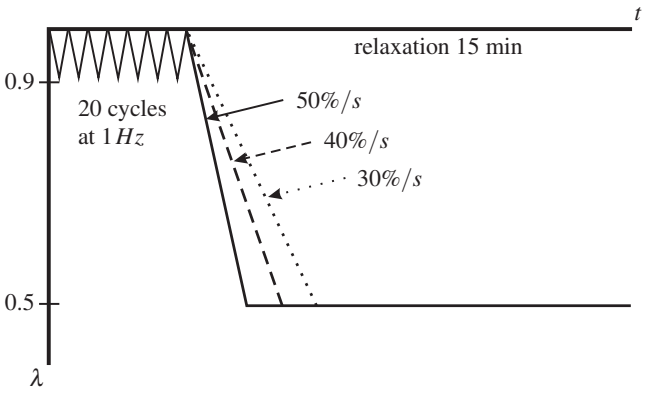

Fig. 3 Scheme of the compression, λ, applied in the relaxation tests.

2.3 Material model

The QLV formulation proposed by Fung [9] was used to model the tissue's mechanical behaviour. In it, the stress response to a step of stretch (or compression) $\lambda = \lambda_0 \cdot H(t)$ (with $H(t)$ the Heaviside function) is factorized in a reduced relaxation function, $\overline{G}(t)$ and an elastic response function, $T^{(e)}(\lambda)$:

$$\sigma(\lambda, t) = \overline{G}(t)\; T^{(e)}(\lambda) \tag{1}$$

For a general stretch history, $\lambda = \lambda(t)$, the stress is given by (see [20] for further details):

$$\sigma(t) = \int_0^t \overline{G}(t-\tau)\; \frac{dT^e[\lambda(\tau)]}{d\lambda}\; \frac{d\lambda(\tau)}{d\tau}\; d\tau \tag{2}$$

This stretch history could be the test performed in the present work (see fig. 3): a ramp of finite strain rate followed by the stress relaxation (the preconditioning cycles will not be considered). With the algorithm applied here to fit the model constants (developed in [20]) the stress relaxation occuring during the ramp is also taken into account and the ramp needs not be very fast to resemble an ideal relaxation test with a step strain. On the contrary, finite and moderate strain rates, of the same order than in1 physiological loads, can be applied.

A fifth-term Prony series was used for $\overline{G}(t)$, like in [12]:

$$\overline{G}(t) = g_\infty + \sum_{i=1}^{5} g_i\, e^{-t/\tau_i} \tag{3}$$

normalized such that:

$$g_\infty + \sum_{i=1}^{5} g_i = 1 \tag{4}$$

The relaxation time constants were taken in decades: $\tau_1 = 0.01\ s$, $\tau_2 = 0.1\ s$, $\tau_3 = 1\ s$, $\tau_4 = 10\ s$ and $\tau_5 = 100\ s$ [10], fixed *a priori* to ensure the uniqueness of the fitted function $\overline{G}(t)$ [21].

The elastic response, $T^{(e)}(\lambda)$, provides the instantaneous stress response to a uniaxial stretch λ and is formulated here using incompressible hyperelastic models. Three models were tried: neo-Hookean ($T^{(e)}_{\mathrm{NH}}$), Mooney-Rivlin ($T^{(e)}_{\mathrm{MR}}$) and an exponential form of the strain energy function ($T^{(e)}_{\mathrm{Expo}}$):

$$T^{(e)}_{\mathrm{NH}} = 2C_{10}(\lambda^2 - \frac{1}{\lambda}) \tag{5a}$$

$$T^{(e)}_{\mathrm{MR}} = 2C_{10}(\lambda^2 - \frac{1}{\lambda}) + 2C_{01}(\lambda - \frac{1}{\lambda^2}) \tag{5b}$$

$$T^{(e)}_{\mathrm{Expo}} = 2\; A\; B\; e^{B(\lambda^2 + \frac{2}{\lambda} - 3)}(\lambda^2 - \frac{1}{\lambda}) \tag{5c}$$

The experimental Cauchy stress was estimated assuming uniaxial compression from the applied force, F, recorded during the test, as:

$$\overline{\sigma}(t) = \frac{F(t)\;\lambda(t)}{A_0}, \qquad \lambda(t) = 1 + \frac{u(t)}{L} \tag{6}$$

where A_0 is the initial cross-sectional area of the sample, $u(t)$ is the displacement of the upper platen, and L is the average thickness.

The evolution of the force applied by the platen, $F(t)$, recorded during the loading ramp in one of the samples is shown in green in figure 4. The typical toe region of soft tissues is seen for small deformations, together with some fluctuations due to the fact that the relative displacement was zeroed when the distance between the platens was equal to the sample's average thickness. At that moment, the upper platen might not be in full contact with the sample, resulting in a spurious toe region. To solve this problem the signal was filtered using a moving average (red dashed line). Nonetheless, the initial slope of the filtered curve was still zero or even positive in some samples. This produced certain numerical problems in the fitting of the experimental stresses to the QLV model. For this reason, an algorithm was developed (see figure 5) to eliminate that spurious toe region.

Placing the upper platen at the average thickness and applying this algorithm was preferred to placing the platen at the minimum thickness, given that it could produce an undesired precompression of the sample.

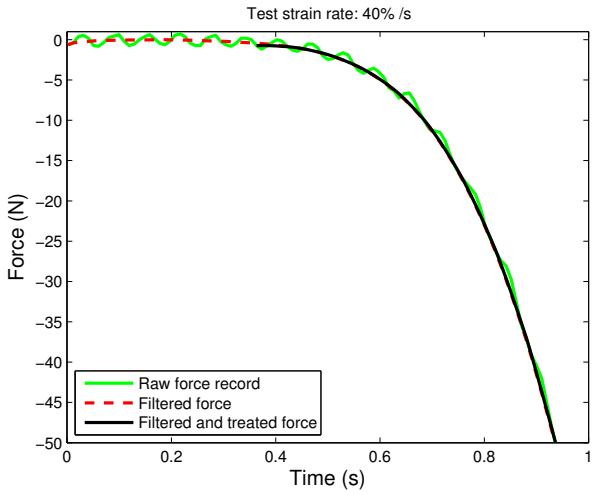

Fig. 4 Comparison of the raw force record (green), the filtered record (red dashed) and the final record after treated with the proposed algorithm to eliminate the spurious toe region (black).

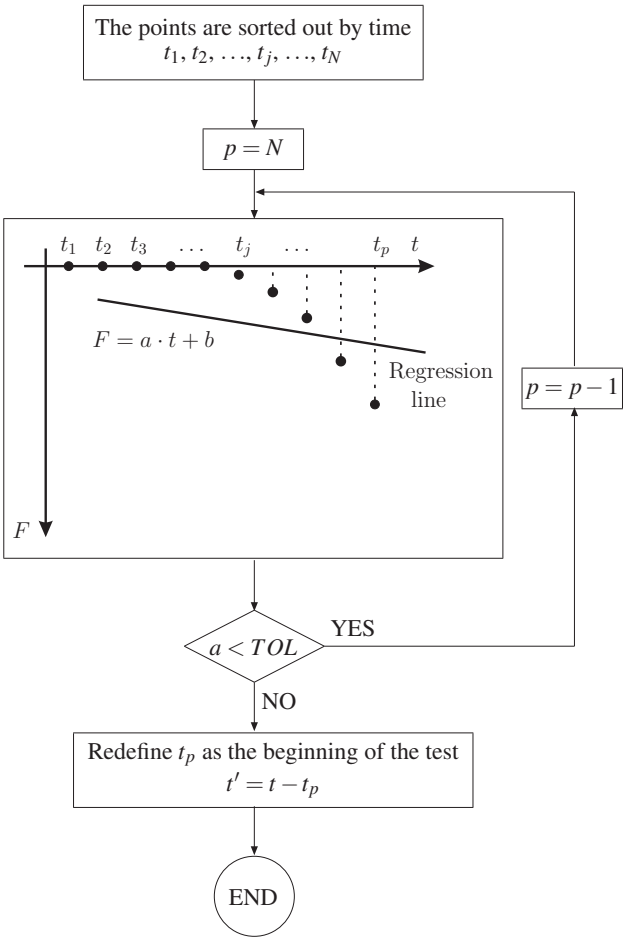

Fig. 5 Algorithm proposed to eliminate the spurious toe region.

With the proposed method, no precompression was induced and the elimination of the spurious toe region, due to an initial lack of contact, was guaranteed.

Once the raw stress record, $\overline{\sigma}$, was filtered and the spurious toe region removed, the resulting stress record, named here $\tilde{\sigma}$, was fitted to the analytical stress record, σ, given by equation (2) using a least squares method, that minimize the following quadratic error:

$$e = \sum_{i=1}^{N} \left(\tilde{\sigma}(t_i) - \sigma(t_i) \right)^2 \tag{7}$$

where N is the total number of points recorded during the relaxation test and t_i is the instant of a certain point. See [20] for further details of how this method was implemented. This least squares method is sensitive to the initial guess in nonlinear problems like this. For this reason, the optimization was performed in two steps. First a genetic algorithm was used to find a minimum of the quadratic error, e, which was used as the initial guess in the second step: the least squares optimization. The genetic algorithm starts with a set of randomly selected potential minima, and makes them evolve by iteratively applying a set of stochastic operators, known as selection, crossover and mutation. This guarantees that the minimum is searched in the entire domain, not only locally. However, genetic algorithms are heuristic methods and the minimum does not necessarily fulfill the optimality condition. This condition was met in the second step, which is a local search around the minimum found in the first step. The goodness of the least squares fitting was evaluated by means of the coefficient of variation, CV:

$$CV(\%) = \frac{\sqrt{\frac{\sum_{i=1}^{N} \left(\sigma(t_i) - \tilde{\sigma}(t_i) \right)^2}{N}}}{\mu_{\tilde{\sigma}}} \times 100 \tag{8}$$

where $\mu_{\overline{\sigma}}$ is the average of the temporal record $\tilde{\sigma}(t_i)$.

3 Results

3.1 Elastic response function

The proposed algorithm was used to fit the QLV model (with different elastic response functions, see eqs. (5)) to the filtered experimental stress record, $\tilde{\sigma}$, of the 45 tested samples. Figure 6 compares a typical experimental stress record with the fitted ones. Figure 7 shows a detail of the stresses during the loading ramp. The stress relaxation was fitted quite accurately in all the cases, though a little better with the exponential model.

The average coefficient of variation, CV, evaluated for the entire record was: 33.35% with the neo-Hookean, 24.90% with the Mooney-Rivlin and 10.52% with the exponential model. However, the loading ramp was highly dependent on the elastic response function. So, when evaluated just in the loading ramp CV was: 96.25% with the neo-Hookean, 74.79% with the Mooney-Rivlin and 25.04% with the exponential model. It can be noticed that the stress increase obtained with the neo-Hookean and Mooney-Rivlin models (as opposed to the exponential model) was not as steep as the real one, resulting in a considerable underestimation of the stress peak. The short term relaxation was also influenced by the elastic response function, indirectly through the stress peak.

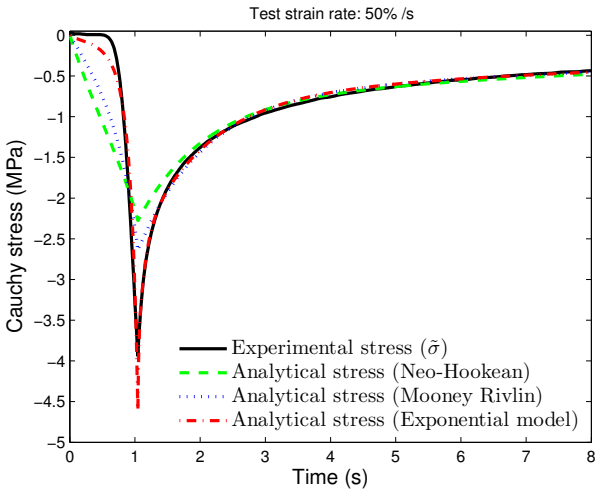

Fig. 6 Example of an experimental stress record fitted with different hyperelastic models.

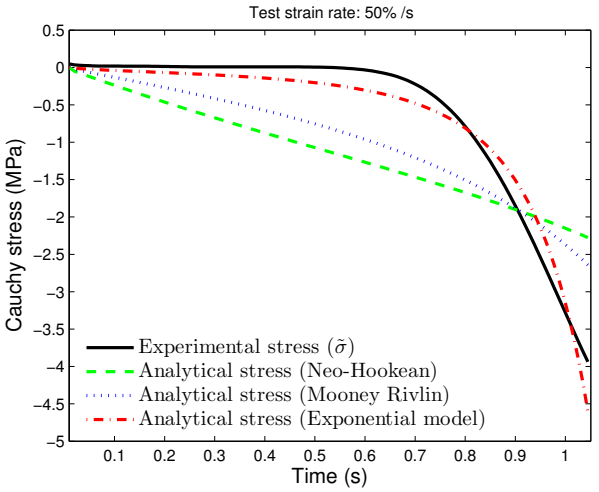

Fig. 7 Detail of figure 6 in the loading ramp.

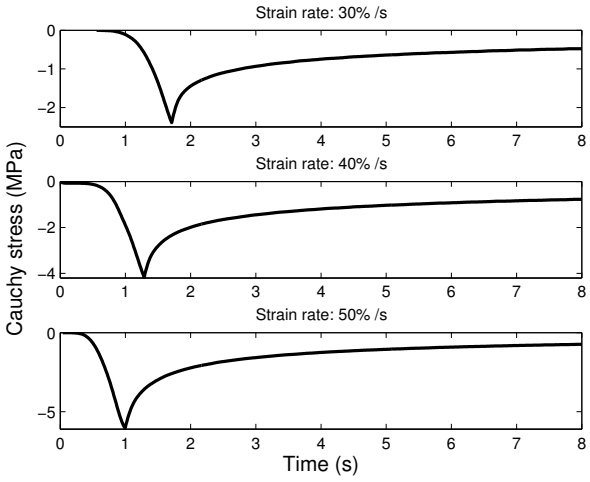

Fig. 8 Example of the experimental stress for each strain rate.

3.2 Validity of QLV

Once it has been shown that the exponential function is more suitable for the elastic response, it has been used in the rest of the paper to show the validity of the QLV approach. As stated before, this must be done by checking that the fitted model constants are independent of the strain rate (given that the independence of the strain level was already checked [16]). Figure 8 shows the filtered stress records obtained in three specimens tested at different strain rates.

To check that the material constants are independent upon the strain rate, a multivariate analysis of variance (MANOVA) was performed, where the independent categorical variable was the strain rate with three levels: 30%/s, 40%/s and 50%/s; and the dependent continuous variables (DVs) were the eight QLV constants: A,B,g_1,g_2,g_3,g_4,g_5,g_∞.

Prior to MANOVA, multivariate outliers were detected. For this purpose, the Mahalanobis distance (MD) was evaluated for each individual. The critical value of this distance is the 99.9% quantile of the χ^2_k, where the number of degrees of freedom ($k = 8$) is the number of DVs. The only individual with $MD \geq \chi^2_{0.999,k} = 26.12$ was removed from the sample. Next, multinormality was checked using the test developed by Cardoso de Oliveira and Ferreira [22]. This test was significant ($p < .001$) and, thus, multinormality was violated, making it necessary to perform a non-parametric MANOVA (NMANOVA).

Table 2 Mean ± standard deviation of the QLV constants using the exponential model for different loading rates.

Loading rate	A (MPa)	B	g_1	g_2	g_3	g_4	g_5	g_∞
30%/s	1.097 ± 1.716	2.547 ± 1.907	0.613 ± 0.190	0.220 ± 0.109	0.114 ± 0.059	0.041 ± 0.020	0.010 ± 0.006	0.003 ± 0.005
40%/s	1.416 ± 1.989	2.547 ± 2.698	0.510 ± 0.208	0.290 ± 0.145	0.134 ± 0.048	0.045 ± 0.020	0.014 ± 0.006	0.007 ± 0.009
50%/s	1.358 ± 1.835	1.959 ± 1.130	0.558 ± 0.174	0.243 ± 0.089	0.131 ± 0.047	0.051 ± 0.030	0.012 ± 0.008	0.005 ± 0.013

MANOVA is indicated if the dependent variables are not correlated. This is not the case for all the variables in this study. For example, A and B are strongly (and negatively) correlated (Spearman $R = -0.772$), and, thus, they can be regarded as the same variable for statistical purposes. The same occurs with g_1, g_2 and g_3, on the one hand, and g_4, g_5 and g_∞ on the other hand. These variables can be grouped. For instance, $g_1 + g_2 + g_3$ and $g_4 + g_5 + g_\infty$ can be, respectively, interpreted as the importance of the short-term and long-term relaxation, in view of (3) and the normalization made in (4). Moreover, those sums are not independent, because of (4). In conclusion, two DVs were compared in the NMANOVA: A and $g_1 + g_2 + g_3$. The NMANOVA test performed was a multivariate extension of the Kruskal-Wallis test, developed by Katz and McSweeney [23]. This test found no significant differences among the three groups compared ($p = .283$). Additionally, a Kruskal-Wallis test was performed on each DV to confirm that conclusion for each of them individually. No significant differences were found in this case either: A ($p = .702$), B ($p = .578$), g_1 ($p = .203$), g_2 ($p = .302$), g_3 ($p = .313$), g_4 ($p = .538$), g_5 ($p = .070$), g_∞ ($p = .052$). Therefore, the hypothesis that the strain rate has no influence on the QLV constants cannot be rejected, at least in the tested range of strain rate.

4 Discussion

During the loading phase of the test, the typical stress-time curve exhibited a toe region followed by a rapid increase of stresses and an approximately linear section. The stress increase was very steep, what made the exponential function the best choice for the elastic response function. The stress relaxation was very quick, with the largest percentage of relaxation occurring in the first 30 seconds and remaining only 0.04% (in average) of the stress peak after one minute. This relaxation rate was much faster and significant than that reported in other soft tissues. In ligaments for example, a maximum relaxation of 31.9% of the stress peak was reported after 60 minutes [24] and in aortic valve leaflets, 55% of relaxation occurred after approximately 30 minutes [13]. Nonetheless, other authors have found the same pattern of quick relaxation for the tissue studied here. Allen and Athanasiou [4] reported a reduction of 75% in the elastic modulus after 30 to 60 seconds in porcine articular disc, though they did not consider the relaxation occurring in the loading ramp, so underestimating the total relaxation.

The fast relaxation resulted in high values of the short-term coefficients, g_1, g_2 and g_3 (see table 2), which weight the importance of relaxation in $\tau_1 = 0.01\,s$, $\tau_2 = 0.1\,s$ and $\tau_2 = 1\,s$, respectively. It must be recalled that the loading ramp spanned from 0 to 1.75 seconds, depending on the loading rate. Therefore, the stress relaxation was significant during the loading ramp making the experiment at those strain rates to be far from an ideal stress relaxation test. Under those conditions it is very important to consider the relaxation during the loading ramp, as the proposed fitting algorithm does [20]. Otherwise, the stiffness of the material would have been strongly underestimated.

Glycosaminoglycans (GAG) content of the porcine TMJ disc is only 1 to 5% of the dry weight [25]. This is quite low compared to articular cartilage. The proteoglycan side chains of many GAGs are hydrophilic. This characteristic can increase the hydrostatic pressure of the interstitial fluid and translate into a higher compressive stiffness. The lack of a significant GAG content in the TMJ disc may be the reason for such short relaxation times. With the sparse scattering of hydrophilic proteoglycans in the extracellular matrix (ECM), interstitial fluid is allowed to flow throughout the ECM with little impedance. The application of compressive strain would pressurize the fluid within the tissue sample. This pressurized fluid initially resists compressive strain and then quickly flows out of the primary collagenous ECM. Mechanically, this would translate into an initial peak load, followed by a fast relaxation represented by low values of τ_i, as obtained here.

The influence of the strain rate on $\overline{G}(t)$ and the constants of the elastic response function was analysed. No statistically significant differences were found in the ma-

terial constants fitted from the tests at different strain rates, at least in the range $30 - 50\%/s$. No significant differences were found either in the constants obtained with different strain levels (25, 30 and 35% strain), as reported in a previous work [16]. Both conclusions support the validity (or, at least, do not lead to a rejection) of the QLV model to describe the viscoelastic behaviour of the disc in the range of strain level and strain rate tested, which include the physiological ranges. Moreover, the exponential strain energy function was much more appropriate for the elastic response function than the neo-Hookean or the Mooney-Rivlin models.

The main limitation of this study is the use of an isotropic model for the articular disc. Certainly, the disc is anisotropic due to its oriented network of collagen fibers. Most of them run in the anteroposterior direction [25], so that they are stretched (contributing with their stiffness) when the disc is compressed in the vertical direction. Under tension, the fibers would be shortened, so not contributing to the overall stiffness. In general, under loads in different directions, the anisotropic behaviour of the disc would be revealed, thus, raising the necessity of an anisotropic model. Nonetheless, this limitation has only a marginal effect, given that the vertical compression applied in the tests is also the predominant type of load during mastication [26, 27], so that the isotropic model fitted from those tests would be valid to characterize the behaviour of the disc during masticatory tasks.

Finally, it must be said that a general validation of the QLV for the TMJ disc would have required the use of a much wider range of strain rates. However the aim of this paper was to show the validity of the QLV model for the physiological range, which is of the same order of magnitude as the strain rates tested here. Indeed, the distance from the condyle to the articular fossa is reduced during mastication between 10 to 20% of the disc's thickness, as estimated in previous FE simulations [28], while the chewing frequency is between 1 and 2 Hz [29].

5 Conclusion

The quasi-linear viscoelastic theory has been widely applied to describe the behavior of ligaments and tendons, since it is a model easier to implement than fully viscoelastic models. However, to the authors' knowledge, it had not been used to describe the behaviour of fibrocartilage. The validity of this model relies on the fulfillment of certain conditions: the independence of the QLV constants on the strain rate (checked in this work) and the strain level (checked in a previous work). Additionally, the strong non-linearity of the observed stress-strain relation, made the exponential strain energy function proposed by Humphrey and Yin for passive cardiac tissue [30] more appropriate for the hyperelastic part of the QLV model than other (simpler) models like neohookean and Mooney-Rivlin.

Another contribution of this work is the algorithm proposed to eliminate the spurious toe region (fig. 5). The toe region is a characteristic feature of the stress-strain curve of soft tissues, but it must be properly captured, because sometimes it can be mixed up with a loss of contact between the sample and the platens. The methodology proposed here has worked correctly to overcome this difficulty.

Acknowledgements Funding was provided by the *Junta de Andalucía* for the research project P07-TEP-03115 entitled *Biomecánica de la mandíbula humana* for which this article has been prepared.

Conflict of interest statement

The authors declare that they have no conflict of interest.

References

1. C.H. Wilkes. Internal derangements of the temporomandibular joint. pathological variations. *Archives of Otolaryngology-Head and Neck Surgery*, 115:469–477, 1989.
2. S. Stankovic, S. Vlajkovic, M. Boskovic, G. Radenkovic, V. Antic, and D. Jevremovic. Morphological and biomechanical features of the temporomandibular joint disc: An overview of recent findings. *Archives of Oral Biology*, 58(10):1475–1482, 2013.
3. E. Tanaka and T. van Eijden. Biomechanical behavior of the temporomandibular joint disc. *Critical Reviews in Oral Biology and Medicine*, 14(2):138–150, 2003.
4. K.D. Allen and K.A. Athanasiou. Viscoelastic characterization of the porcine temporomandibular joint disc under unconfined compression. *Journal of Biomechanics*, 39(5):312–322, 2006.
5. L.P.Y Chin, F.D. Aker, and K. Zarrinnia. The viscoelastic properties of the human temporomandibular joint disc. *Journal of Oral Maxillofacial Surgery*, 54:315–318, 1996.
6. M. Beek, M.P. Aarnts, J.H. Koolstra, A.J. Feilzer, and T.M.G.J. van Eijden. Dynamical properties of the human temporomandibular joint disc. *Journal of Dental Research*, 80 (3):876–880, 2001.
7. R. del Pozo, E. Tanaka, M. Tanaka, M. Okazaki, and K. Tanne. The regional difference of viscoelastic property of bovine temporomandibular joint disc in compressive stress-relaxation. *Medical Engineering and Physics*, 24:165–171, 2002.
8. E. Tanaka, M. Tanaka, Y. Miyawaki, and K. Tanne. Viscoelastic properties of canine temporomandibular joint disc in compressive load-relaxation. *Archives of Oral Biology*, 44:1021–1026, 1999.

9. Y.C. Fung. *Biomechanics: Mechanical properties of living tissues*. Spinger-Verlag, New York, 1993.
10. J.H. Koolstra, E. Tanaka, and T.M.G.J. van Eijden. Viscoelastic material model for the temporomandibular joint disc derived from dynamic shear test or strain relaxation tests. *Journal of Biomechanics*, 40:2330–2334, 2007.
11. E. Tanaka, K. Hanaoka, T.M. van Eijden, M. Tanaka, M. Watanabe, N. Nishi, and et al. Dynamic shear properties of the temporomandibular joint disc. *Journal of Dental Research*, 82:228–231, 2003.
12. M.J. Lamela, Y. Prado, P. Fernandez, A. Fernández-Canteli, and E. Tanaka. Non-linear viscoelastic model for behavior characterization of temporomandibular joint discs. *Experimental Mechanics*, 51:1453–1440, 2011.
13. E.O. Carew, E.A. Talman, D.R. Boughner, and I. Vesely. Quasi-linear viscoelastic theory applied to internal shearing of porcine aortic valve leaflets. *Journal of Biomechanical Engineering*, 121:386–392, 1999.
14. C.S. Drapaca, G. Tenti, K. Rohlf, and S. Sivaloganathan. A quasi-linear viscoelastic constitutive equation for the brain: Application to hydrocephalus. *Journal of Elasticity*, 85:65–83, 2006.
15. S.L-Y. Woo, B.R. Simon, S.C. Kuej, and W.H. Akeson. Quasi-linear viscoelastic properties of normal cartilage. *Journal of Biomechanical Engineering*, 102:85–90, 1980.
16. M.S. Commisso. *Biomechanics of the human mandible including the temporomandibular joint*. PhD thesis, University of Seville, 2012.
17. M.S. Commisso, J. Martínez-Reina, J. Mayo, J. Domínguez, and E. Tanaka. Effect of non-uniform thickness of samples in stress relaxation tests under unconfined compression of samples of articular discs. *Journal of Biomechanics*, 47 (6):1526–1530, 2014.
18. G.N. Kiefer, K. Sundby, D. McAllister, N.G. Shrive, C.B. Frank, T. Lam, and N.S. Schachar. The effect of cryopreservation on the biomechanical behaviour of bovine articular cartilage. *Journal of Orthopedic Research*, 7(4):494–501, 1989.
19. M. Hongo, R.E. Gray, J.T. Hsu, K.D. Zhao, B. Ilharreborde, L.J. Berglund, and K.N. An. Effect of multiple freeze-thaw cycles on intervertebral dynamics motion characterisitics in the porcine lumbar spine. *Journal of Biomechanics*, 41(4):916–920, 2008.
20. Commisso M.S., J. Martínez-Reina, J. Mayo, and et al. Numerical simulation of a relaxation test designed to fit a quasi-linear viscoelastic model for temporomandibular joint discs. *Proc I Mech E Part H: J Eng Med*, 227(2):190–199, 2013.
21. K.L. Troyer, D.J. Estep, and C.M. Puttlitz. Viscoelastic effects during loading play an integral role in soft tissue mechanics. *Acta Biomaterialia*, 8:234–243, 2012.
22. I.R. Cardoso de Oliveira and D.F. Ferreira. Multivariate extension of chi-squared univariate normality test. *Journal of Statistical Computation and Simulation*, 80(5):513–526, 2010.
23. B.M. Katz and M. McSweeney. A multivariate kruskal-wallis test with post hoc procedures. *Multivariate Behavioral Research*, 15:281–297, 1980.
24. S.D. Abramowitch and S.L-Y. Woo. An improved method to analyze the stress relaxation of ligaments following a finite ramp time based on the quasi-linear viscoelastic theory. *Journal of Biomechanical Engineering*, 126:92–97, 2004.
25. M.S. Detamore and K.A. Athanasiou. Structure and function of the temporomandibular joint disc:implications for tissue engineering. *Journal of Oral Maxillofacial Surgery*, 61:494–506, 2003.
26. M.S. Commisso, J. Martínez-Reina, and J. Mayo. A study of the temporomandibular joint during bruxism. *International Journal of Oral Science*, 2014.
27. J.H. Koolstra and T.M.G.J. van Eijden. Combined finite-element and rigid-body analysis of human jaw joint dynamics. *Journal of Biomechanics*, 38:2431–2439, 2005.
28. Commisso M.S., J. Martínez-Reina, J. Ojeda, and J. Mayo. Finite element analysis of the human mastication cycle. *Journal of the Mechanical Behavior of Biomedical Materials*, 41:23–35, 2015.
29. Po J.M., Kieser J.A., Gallo L.M., Tésenyi A.J., Herbison P., and Farella M. Time-frequency analysis of chewing activity in the natural environment. *Journal of Dental Research*, 90 (10):1206–1210, 2011.
30. J.D. Humphrey and F.C.P. Yin. On constitutive relations and finite deformations of passive cardiac tissue: I a pseudostatic energy function. *ASME Journal of Biomechanical Engineering*, 109:298–304, 1987.